Application of Differential Scanning Calorimetry (DSC) in study of phase transformations in ductile iron

R. Przeliorz, J. Piątkowski*

Chair of Materials Technology, Silesian University of Technology, Krasińskiego 8, 40-019 Katowice, Poland
*Corresponding author. E-mail address: jaroslaw.piatkowski@polsl.pl

Abstract

The effect of heating rate on phase transformations to austenite range in ductile iron of the EN-GJS-450-10 grade was investigated. For studies of phase transformations, the technique of differential scanning calorimetry (DSC) was used. Microstructure was examined by optical microscopy. The calorimetric examinations have proved that on heating three transformations occur in this grade of ductile iron, viz. magnetic transformation at the Curie temperature, pearlite→austenite transformation and ferrite→austenite transformation. An increase in the heating rate shifts the pearlite→austenite and ferrite→austenite transformations to higher temperature range. At the heating rate of 5 and 15°C/min, local extrema have been observed to occur: for pearlite→austenite transformation at 784°C and 795°C, respectively, and for ferrite→austenite transformation at 805°C and 821°C, respectively. The Curie temperature of magnetic transformation was extrapolated to a value of 740°C. Each transformation is related with a specific thermal effect. The highest value of enthalpy is accompanying the ferrite→austenite transformation, the lowest occurs in the case of pearlite→austenite transformation.

Keywords: Theoretical Fundamentals of Crystallisation Process, Inoculation, Ductile Iron

1. Introduction

Ductile iron is an engineering material for various applications [1÷4]. One of the most important advantages it offers is the possibility of shaping its mechanical properties by heat treatment. Therefore numerous research centres carry out investigations on the kinetics of phase transformations and, consequently, on the improvement of cast iron properties. Most of the research is, however, focussed on the analysis of phase transformations taking place on cooling. Only few studies are devoted to the analysis of effects that take place during heating and austenitising [5÷7]. The mechanical properties of cast iron, i.e. the tensile strength, elongation and hardness, largely depend on the cast iron structure in initial condition, i.e. upon casting solidification, and on changes that take place in this structure after the successive operations of heat treatment.

The thermal energy supplied on heating of cast iron causes phase transformations, changes the solubility of phase constituents and caloric properties, like heat capacity, heat conductivity, and temperature compensation factor. The technique often used to measure the temperature and enthalpy of phase transformations is differential scanning calorimetry (DSC). The DSC method measures the difference in the amount of heat supplied to the examined sample and to a reference sample, when both are subjected to controlled changes of temperature. The measured signal, i.e. the surface area under the thermal effect on a heat flux – time curve, is directly proportional to the amount of heat absorbed or emitted [8].

One of the most important conditions in DSC measurements is calibration of heat flux and temperature. It is generally assumed that the thermal equilibrium in a measuring system (sample, container for samples, reference sample) can be achieved only in some approximation. Moreover, as follows from the design of a DSC measuring system, the heat flux cannot be measured directly in the sample. To obtain true values of the heat flux, used next in the quantitative measurements, different calibration methods are applied, e.g. a stepwise method, a discrete method [9÷12].

The aim of the present study was to determine the applicability of the differential scanning calorimetry in quantitative analysis of the temperature and enthalpy of phase transformations that occur in industrial ductile iron castings. The influence of the heating rate on the position of the thermal effects of phase transformations and on the degree of pearlite → austenite and ferrite → austenite transformation during heating to the point of austenitisation was also examined.

2. Test methods

Studies were carried out on commercial ductile iron of the EN-GJS-450-10 (PN-EN 1563: 2000) grade. The cast iron is used for slot grids operating in a linear water disposal system. Table 1 gives the chemical composition of cast iron. In as-cast condition, the cast iron matrix is ferritic with spheroidal graphite. The microstructure also includes pearlite (Fig. 1).

Table 1.
The chemical composition of cast iron

Content of element in, % weight							
C	Si	Mn	P	S	Cr	Mg	Fe
3,55	2,5	0,6	0,02	0,008	0,03	0,017	93,2

The calorimetric measurements were carried out on cylindrical specimens of d = 3, h = 4 mm. For measurements, a high-temperature M HTC S60 Setaram calorimeter was used The specimens were placed in an alumina crucible of 0,45 cm^3 capacity and were preheated to 950°C. The reference material was Al_2O_3. The analysis was made in argon. Two heating rates were applied, i.e. 5 and 15°C/min.

The energy and temperature were calibrated following the instructions given in a calorimeter service manual. Five metallic reference samples were used, i.e. In, Al, Ag, Au, Ni. Each reference sample was heated at a rate of 2, 10 and 15°C/min. The calibration coefficient K_i at the melting point T_{top} was calculated from the following formula:

$$K_i = \frac{S_i}{H_i} \cdot \frac{1}{m}, \mu V / W \tag{1}$$

where:
S_i- the surface area of thermal effect, µV·s,
H_i- the enthalpy of reference sample melting, J/g,
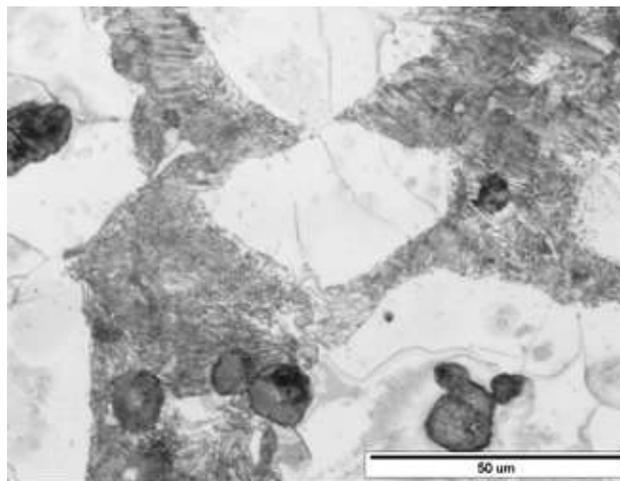m- the weight of the examined reference sample, g.

Fig. 1. Ductile iron microstructure. Spheroidal graphite in ferritic matrix with precipitates of pearlite. Etched with 3% Nital

For example, the calibration coefficient of aluminium is:

$$K_{Al} = \frac{23,81, \mu V \cdot s}{395,5, J/g} \cdot \frac{1}{150 \cdot 10^{-3}, g} = 0,4013, \mu V / mW \tag{2}$$

The heat calibration curve plotted for a Multi HTC differential calorimeter in function of temperature is shown in Fig. 2. It is recommended to describe the curve with a fourth-degree polynomial. The coefficients A_0, A_1, A_2, A_3, A_4 entered into the parameters software are transformed into thermal power signals. The integration of peaks yields directly the heat value in joules. For an arbitrary thermal effect of the surface area A (µV·s), the transformation heat Q (J) is computed from the following formula:

$$Q = A/K \tag{3}$$

In practice, the calibration of temperature and energy is made in the same experiment and for the same reference sample.
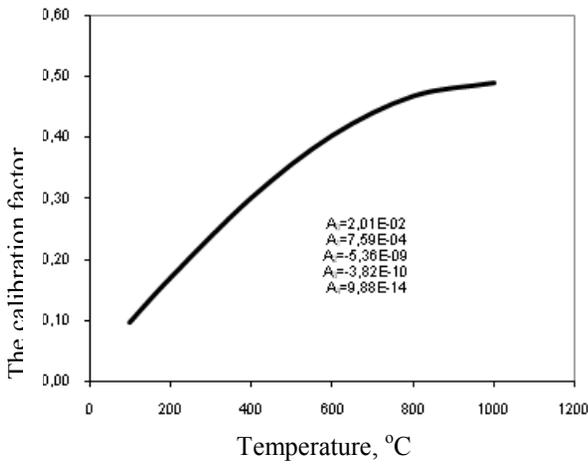

Fig. 2. The heat calibration curve as a function of temperature

3. The results and analysis

The process of ductile iron heating is of a complex character, and this is mainly due to the formation of different phases, which can successively change and transform into one another. Moreover, a characteristic feature of the iron-graphite system is that it may contain mono-phase constituents (α, γ, Fe_3C, $C_{graphite}$), two-phase constituents (ledeburite, pearlite), and multi-phase constituents of variable composition (phosphorus eutectic, sulphate complexes). This is why the methods that examine the process as one integral whole are not suitable in investigations of the mechanism that drives the transformations, the more that sometimes the thermal effects can overlap on the DSC curve.

The calorimetric investigations have proved that on heating to austenite range, three endothermic transformations take place in the ductile iron (Figs. 3 and 4).
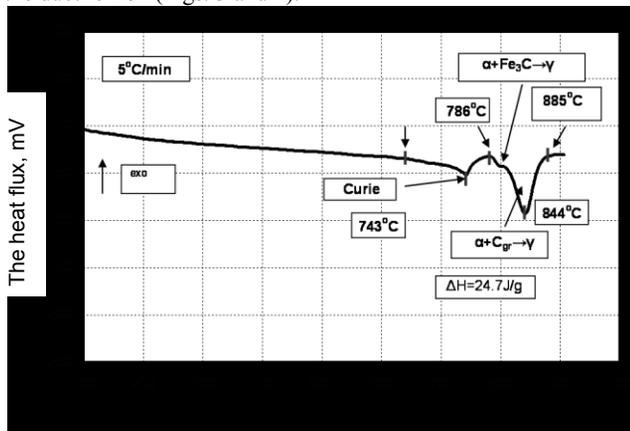

Fig. 3. The DSC curve of ductile iron. The applied heating rate was 5°C/min

The first endothermic effect, which appears on the DSC curve at a heating rate of 5°C/min (Fig. 3), has an extremum at the temperature of 743°C. This effect is related with magnetic transformation at the Curie temperature. With the heating rate increased to 15°C/min, the local minimum of the Curie transformation shifts to higher temperatures, i.e. 753°C (Fig. 4).
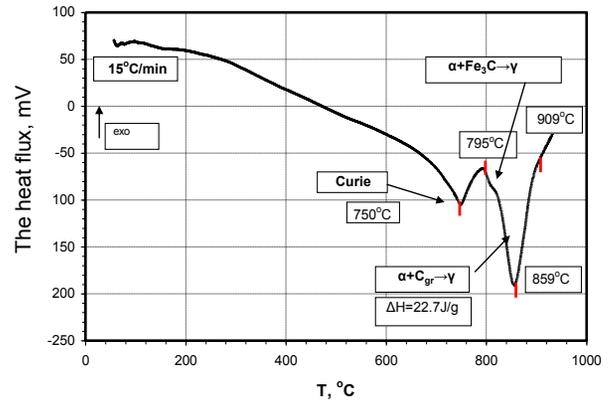

Fig. 4. The DSC curve of ductile iron. The applied heating rate was 15°C/min

The second endothermic effect, which results from the pearlite → austenite transformation, is partly overlapping the ferrite → austenite transformation. Therefore it was not possible to determine exactly the temperature of the end of the transformation of eutectoid into austenite and of the beginning of the transformation of ferrite into austenite. So, it has been assumed that the temperature of the end of pearlite → austenite transformation is at the same time the temperature of the beginning of ferrite → austenite transformation. In the examined cast iron, the temperature range of pearlite → austenite transformation was 784÷805°C and 795÷821°C for the heating rates of 5°C/min and 15°C/min, respectively. The thermal effect of the reaction seemed to be inversely proportional to the heating rate. At a lower heating rate, i.e. at 5°C/min, the enthalpy of the transformation was 0,46 J/g, while at a heating rate of 15°C/min it amounted to 0,14 J/g only. With higher heating rates, an obvious blurring of the shape of this effect has occurred (Fig. 5).
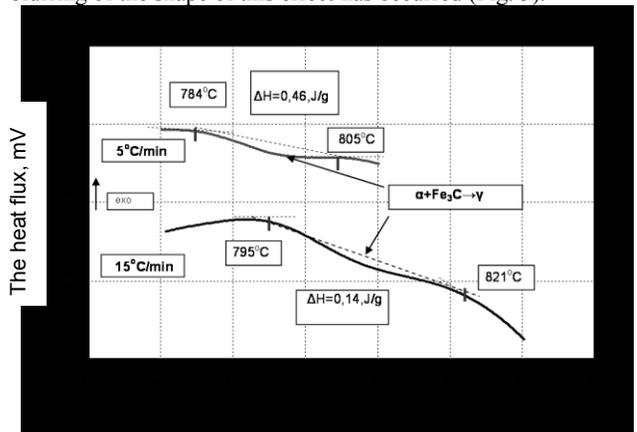

Fig. 5. A fragment of the DSC curve. Visible is the pearlite → austenite transformation

Table 2 gives the characteristic transformation temperatures with the corresponding values of enthalpy.

Table 2.
Characteristic transformation temperatures

Transfor-mation	Temperature, °C			Enthalpy ΔH, J/g	Heating rate, °C/min
	T_p	T_{max}	T_K		
Curie		743			
$\alpha+Fe_3C \rightarrow \gamma$	784	796	805	0,46	5
$\alpha+C_{gr} \rightarrow \gamma$	805	844	885	24,7	
Curie		750			
$\alpha+Fe_3C \rightarrow \gamma$	795	809	821	0,14	15
$\alpha+C_{gr} \rightarrow \gamma$	821	859	909	22,7	

The third endothermic effect is due to ferrite → austenite transformation. Depending on the heating rate, the temperature range was 805÷885°C or 821÷909°C. Among all the examined reactions, the ferrite → austenite transformation was accompanied by the strongest thermal effect. The value of the transformation enthalpy was ΔH = 24,7 J/g and 22,7 J/g for the heating rates of 5°C/min and 15°C/min, respectively. The total thermal effect of the pearlite→austenite and austenite →ferrite transformations was similar and amounted to 25,2 J/g and 22,8 J/g, respectively.

4. Discussion of results

The phase transformations that take place in ductile iron on heating to the point of austenitisation are of a complex character. The DSC curve shows the presence of three phase transformations:
- a ferromagnetic → paramagnetic transformation at the Curie point,
- a pearlitic transformation during which the eutectoid changes into austenite according to the reaction:

$$\alpha + Fe_3C \rightarrow \gamma_P \tag{4}$$

- a solid-state transformation of ferrite into austenite accompanied by partial dissolution of carbon contained in graphite

$$\alpha + C_{gr} \rightarrow \gamma_F \tag{5}$$
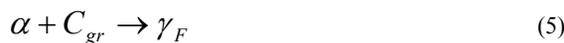
where: γ_P and γ_F - is the austenite formed as a result of pearlite and ferrite transformation, respectively.

Each of the transformations takes place within a different range of temperatures and has different values of the enthalpy. Contrary to transformations of the first kind (melting, solidification, evaporation, polymorphous transformations), in phase transformations of the second kind, which include the Curie

point transition from ferromagnetic to paramagnetic state, the absorption or emission of heat does not occur. These transformations are running accompanied by a number of the successively occurring small stepwise changes, which take place within predetermined temperature ranges. Due to this, they resemble a continuous process, though formally are of a discrete nature. For the examined cast iron, the Curie temperature of transformation was extrapolated to a value of 740°C. From Figures 3 and 4 and from Table 2 it follows that the magnetic transformation is much less sensible to the effect of the heating rate than other transformations are. In pure α (alpha) iron, the ferromagnetism disappears at a temperature of 769°C. It is generally considered that shifting of the Curie temperature in cast iron to a lower level is the result of silicon dissolving in ferrite [5, 14]. The effect of heating rate is important for the pearlite → austenite and ferrite → austenite transformations. At a lower heating rate, the shape of the endothermic effect is much more distinct (Figs. 3 and 4). At the same time, the amount of the absorbed heat is higher than it is when the heating rate is 15°C/min (Table 2). This is due to a specific character of the eutectoid transformation. The eutectoid transformation is of a diffusive character and, besides temperature, time is the main factor here. It starts with the formation of austenite nuclei at the ferrite/cementite lamellae interface. Because of an allotropic transformation of α (alpha) iron into γ (gamma) iron, the nuclei of austenite are growing and fill the whole grain of pearlite. The allotropic α → γ transformation is proceeding at a higher rate than the dissolution of cementite [12, 15]. Therefore, when ferrite exists no longer, there is still cementite to dissolve gradually in austenite. At the beginning, the austenite in the grains is non-homogeneous because of higher carbon content in places where the cementite is present. The homogenisation of austenite begins only after a lapse of time. According to [5], the non-homogeneity of austenite extends the range of pearlite→austenite transformation and, as a consequence of this situation, overlapping of thermal effects of the pearlite → austenite and ferrite → austenite transformations occurs.
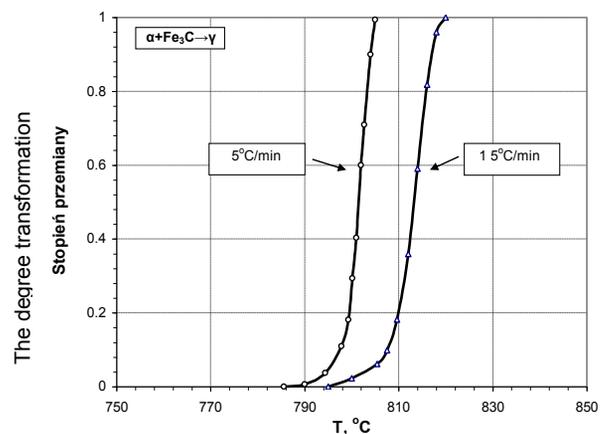

Fig. 6. The degree of pearlite→austenite transformation computed in function of the heating rate

The kinetics of the examined transformations is shown in Fig. 7. The computations are based on equation (1) and on the

assumption that the degree of transformation is proportional to the magnitude of the thermal effect [5]:

$$f(t) = \frac{\int_{T_S}^{T} \frac{\partial h}{\partial t} dt}{\int_{T_s}^{T_E} \frac{\partial h}{\partial t} dt} = \frac{\int_{T_S}^{T} H dt}{\int_{T_s}^{T_E} H dt} \qquad (6)$$

where:
f(t) – the fraction of transformation completed in a given time unit (t),
(H) – the heat flux from the beginning to the end of transformation.

From the kinetic curves it follows that the temperature range for pearlite → austenite transformation is much narrower than the temperature range within which the ferrite → austenite transformation occurs. Moreover, an increase in the heating rate shifts the transformation to higher temperatures and extends the temperature range. The temperature range of pearlite → austenite transformation is 785÷805°C and 795÷820°C for the heating rates of 5 and 15°C, respectively. The same tendency was observed in ferrite → austenite transformation, though in this case the range of the transformation temperatures was higher and amounted to 805÷885°C and 820÷910°C, respectively. As might be expected, in this case, the value of the transformation enthalpy was similar for different heating rates.
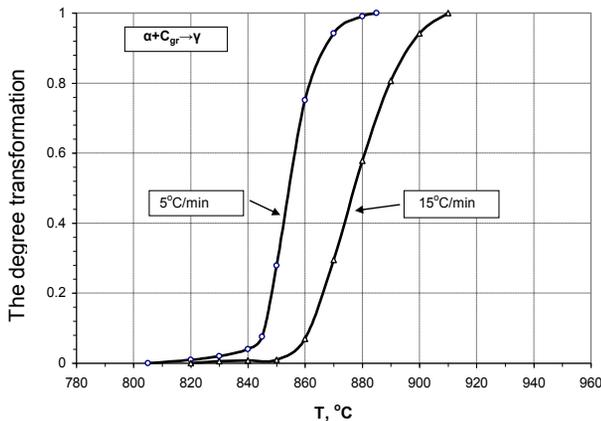

Fig. 7. The degree of ferrite→austenite transformation computed in function of the heating rate

5. Conclusions

– Heating of ferritic ductile iron to the temperature range of austenite stability is of a complex character and proceeds at three stages. These are the following transformations: ferromagnetic-to-paramagnetic transformation at the Curie point, pearlite-to-austenite transformation, and ferrite-to-austenite transformation. The transformations are accompanied by an endothermic effect.
– An increase in the heating rate shifts the transformation temperature to a higher range of values. The Curie transformation temperature at a heating rate of 5 and 15°C/min is 743°C and 753°C, respectively. The effect of the changing heating rate is more visible in pearlite → austenite and ferrite → austenite transformations. The temperature range of the eutectoid transformation is 784÷805°C and 795÷821°C for the heating rates of 5 and 15°C/min, respectively. For the same heating rates, the temperature of the ferrite → austenite transformation amounts to 805÷885°C and 821÷909°C, respectively.
– The scanning differential calorimetry is an effective tool in the investigation of phase transformations taking place in ductile iron. It enables very accurate determination of the temperature range and reaction heat in all transformations, the magnetic one included.

References

[1] Y. Zhou, Z. Lu , M. Zhan, An Investigation of the Erosion–Corrosion Characteristics of Ductile Cast Iron, Materials and Design 28 (2007), 260–265
[2] T. Gren , I.L. Svensson, The Effect of Graphite Fraction and Morphology on the Plastic Deformation Behavior of Cast Irons, The Minerals, Metals & Materials Society and ASM International 2007, 840, Vol. 38A, April 2007
[3] Z. L. Lu, Y.X., Zhou, Q.Ch Rao, Z.H. Jin, An Investigation of the Abrasive wear Behavior of Ductile Cast Iron, Journal of Materials Processing Technology 116 (2001), 176-181
[4] C. Labrecque, M. Gagne, Review Ductile Iron, Canadian Metallur`ical Quarterly, Vol. 26 No. 4, 232-267, 0887
[5] R. Ivanova, W. Sha, S. Malinov, Differential Scanning Calorimetry and Microscopy Study of Transformations in Ductile Cast Irons: Part I Continuous Hetaing, ISIJ International, Vol. 44 (2004), No. 5, 886–895
[6] R.C. Thomson, J. S. James, D.C. Putman, Mater. Sci. Technol. 16 (2000), 1412
[7] O.M. Suares, C.R. Loper, Metall. Mater. Trans. A. 32A (2001), 2131
[8] A.T.W. Kempen., F. Sommer., E.J. Mittemeijer., Calibration and desmearing of differential thermal analysis measurement signal upon heating and cooling, Thermochimica Acta 383 (2002), 21-30
[9] G.W.H. Höhne, W. Hemminger, H.J. Flammersheim, Differential Scanning Calorimetry, Springer-Verlag, Berlin 1996
[10] K. L. Ramakumar, M. K. Saxena and S. B. Deb, Experimental Evaluation of Procedures for Heat Capacity Measurement by Differential Scanning Calorimetry, Journal of Thermal Analysis and Calorimetry, Vol. 66 (2001), 387-397
[11] V. A. Drebushchak, Calibration Coefficient of Heat-Flow DSC, Journal of Thermal Analysis and Calorimetry, Vol. 76 (2004), 941-947

[12] K. Das, T.K. Bandyopadhyay, Application of Differential Scanning Calorimetry (DSC) Kinetic Methods to Determine the Kinetic Parameters of α Precipitation in A 60/40 brass, Scripta mater. 44 (2001) 2597–2603

[13] E. Linares, V. Gerval, J. Lacaze, On the Characteristic Temperatures of the Eutectoid Reaction in Cast Irons, Scripta Materialia, Vol. 38. No. 2, pp. 279-285, 1998

[14] Yuan W.J.,Li R,. Shen Q,. Zhang L.M, Characterization of the evaluation of the solid solubility of Si in sintered Fe–Si alloys using DSC technique, Materials Characterization 58 (2007) 376–379

[15] Liu Y.C, Sommer F.,. Mittemeijer E.J, The austenite–ferrite transformation of ultralow-carbon Fe–C alloy; transition from diffusion- to interface-controlled growth, Acta Materialia 54 (2006) 3383–3393